Shared Blood Transcriptomic Signatures between Alzheimer's Disease and Diabetes Mellitus

(Supplementary Material)

Taesic Lee[1] and Hyunju Lee[1, 2, 3]

[1]Department of Biomedical Science and Engineering, Gwangju Institute of Science and Technology, Gwangju, South Korea.

[2]Artificial Intelligence Graduate School, Gwangju Institute of Science and Technology, Gwangju, South Korea.

[3]School of Electrical Engineering and Computer Science, Gwangju Institute of Science and Technology, Gwangju, South Korea.

Corresponding author

Hyunju Lee, PhD

Professor, School of Electrical Engineering and Computer Science

Artificial Intelligence Graduate School

Gwangju institute of science and technology

Selection of Appendicitis as the control disease (For 2.1 section in Manuscript)

To select control disease irrelevant with AD, we used the two disease-disease networks, including the human symptom disease network (HSDN) [1] and interactome-separation network (ISN) [2, 3]. HSDN estimated relationship between two diseases via cosine similarity of Term Frequency-Inverse Document Frequency of symptom values that were previously curated from PubMed [1]. For ISN, we used disease-related genes curated from DigSee [3] and PPI network [2], constructed disease modules, and calculated the degree of relationship between two diseases via modular distance. As a result, 146 diseases [i.e., cholangitis, diverticulitis, and appendicitis (AP)] were resulted to be irrelevant with AD in both HSDN and ISN.

Preprocessing of blood RNA datasets (For 2.1 section in Manuscript)

We downloaded ADNI expression data normalized by Robust Multi-Array Analysis (RMA) method [4]. We downloaded normalized datasets (Accession ID: GSE63060 and GSE63061) from the Gene Expression Omnibus database (GEO) [5]. We downloaded “GSE85426 raw data.txt" from the GEO, then scaled and normalized GSE85426 via exponential function and quantile normalization (normalizeQuantiles function in limma package), respectively.

E-MTAB-6667 was normalized by background correction and quantile normalization via ‘neqc’ function in lumi package. We used RNA expression data (E-MTAB-6667) of CD14 positive blood samples. Because E-MTAB-6667 included the unbalanced number of samples (19 diabetes mellitus (DM) patients and 291 healthy controls), we resampled 40 subjects among 291 healthy controls without replacement. We iterated the resampling at 100 times, and in each iteration, we measured Spearman’s correlation coefficient value between log[fold change (FC)] values for all genes between two conditions of the original dataset and those of resampled dataset. The logFC values were RNA expression alteration between control and DM, measured by Limma method [6]. The number of logFC values were same with the number of genes in RNA expression set (i.e., if a RNA expression data consists of N number of genes, we can get N number of FC values). We selected a resampled dataset with the highest correlation value (Spearman correlation coefficient = 0.9894).

We downloaded GSE87005 pre-processed by the locally weighted scatterplot smoothing (LOWESS) algorithm [7], and normalized the downloaded dataset via quantile normalization (normalizeQuantiles function in limma package). GSE23561 was normalized by quantile normalization (normalizeQuantiles function in limma package). We scaled and normalized GSE9006 via log transformation and quantile normalization (normalizeQuantiles function in limma package), respectively.

We scaled and normalized GSE9579 (# of controls = 4, # of AP = 9) via log transformation and quantile normalization (normalizeQuantiles function in limma package), respectively.

For all RNA expression datasets, we excluded approximately 30% of the probes that had small standard deviations across samples, then about 30% of the under-expressed probes based on the small mean expression values across subjects. To systemically compare gene expression of different platforms, we mapped all probes or probe-sets ID to Entrez ID, and we eliminated probes without matched Entrez IDs. For multiple probes annotated with a gene (Entrez ID), we selected the probe with the maximum average expression value via 'collapseRows' function in Weighted Gene Co-Expression Network Analysis (WGCNA) package[8].

MetaQC (For 2.2 section in Manuscript)

Using the 'MetaQC' and 'runQC' functions in the MetaQC package, we calculated the levels of the six QC indices and SMR for each RNA expression dataset. Because pathway information was needed to measure the six QC indices in MetaQC, we downloaded the Kyoto Encyclopedia of Genes and Genomes (KEGG)[9] database from MSigDB[10] To run the MetaQC algorithm, at least three RNA datasets were needed. If we had used the MetaQC method to analyze four RNA datasets for each disease, only 1000 to 2000 genes would have been available for measuring QC, because only genes that were present across all studies were analyzed. Therefore, each time, we measured the QC of three RNA datasets that were the minimum size required to run the MetaQC. As a result, four combinations $[{}_{4\text{(four AD or DM RNA datasets)}}C_{3\text{(minimum number of sets for MetaQC)}}]$ of the MetaQC were calculated.

Permutation test (For 2.4 section in Manuscript)

For each study (AD, DM, and AP), we randomly permuted case/control status at 20,000 times and repeated the differential expression analysis (logFC between two randomly assigned group) using limma, yielding a null distribution consisting of 20000 of Spearman's correlation coefficients. The permutated p-value was determined as follows:

$$P-value = \frac{\text{\# of cases (Correlation coefficient of permuted status} > \text{Correlation coefficient of actual status)}}{\text{20000 (iteration time), a null distribution}}$$

Hyper-parameters for rWGCNA (For 2.5 section in Manuscript, Fig.S1, and Fig.S2)

A robust version of Weighted Gene Co-Expression Network Analysis (rWGCNA) [11, 12] was used to minimize the influence of potential outlier samples with the biweight midcorrelation (bicor). For

the co-expression network, a signed network was used, with a soft-threshold power of 9 to achieve approximate scale-free topology ($R^2 > 0.8$, Fig.S1). The network dendrogram was created by using average linkage hierarchical clustering of the topological overlap dissimilarity matrix (1 − TOM). Modules were defined as branches of the dendrogram using the hybrid dynamic tree-cutting method [13]. We set the pamStage as "False". We iterated construction of co-expression network at 40 times as setting different hyper-parameters, and selected a case with consisting modules that were conserved during different setting with ratio of 0.25. In other words, all modules in the selected case were curated at more than 10 times among 40 simulations. Finally, we determined a consensus quantile threshold, a minimum module size, deepsplit, and pamStage as 0.1, 100, and 1, respectively.

Measurement of differential connectivity (For 2.5 section)

The differential connectivity was measured as following steps.

Step 1) Given gene i and gene j, we calculated $k_{ij} = |cor(i,j)|^{\beta}$, with defining k, cor (), and β as connectivity, biweight midcorrelation, and hyper-parameter (named as soft-threshold power) determined by researcher, respectively.

Step 2) We measured the mean connectivity (MC) of gene i with other genes in a module consisting of N genes, as $MC_i = \sum_{j=1}^{N} k_{ij(i\neq j)}$. Then, using RNA expression data of disease samples, we measured MCs of N genes ($MC_{1\ N}^{Disease(Dx)} = MC_1^{Dx}, MC_2^{Dx}, MC_3^{Dx}, \cdots, MC_N^{Dx}$), and using those of control samples, we also calculate MC of N genes ($MC_{1\ N}^{Control}$). We compared $MC_{1\ N}^{Disease}$ and $MC_{1\ N}^{Control}$ using t-test, and selected a module with Bonferroni-corrected p-value < 0.05, and named the module as the module with modular differential connectivity (MDC).

Preprocessing of brain and fat RNA expression datasets (For 3.7 section in Manuscript)

We downloaded GSE5281 and GSE20966 dataset from the GEO DB [5]. Then we scaled and normalized the two datasets via log transformation and quantile normalization, respectively. We mapped probe ID to Entrez ID, and removed probes without a matched-Entrez ID. Afterward, we excluded approximately 30% of the probes that had small variance across samples. For multiple probes mapped with a gene (Entrez ID), we selected the probe with the maximum average expression value via 'collapseRows' function in WGCNA package [8].

References

1. Zhou, X., et al., Human symptoms-disease network. Nat Commun, 2014. 5: p. 4212.

2. Menche, J., et al., Disease networks. Uncovering disease-disease relationships through the incomplete interactome. Science, 2015. 347(6224): p. 1257601.

3. Kim, J., J.J. Kim, and H. Lee, An analysis of disease-gene relationship from Medline abstracts by DigSee. Sci Rep, 2017. 7: p. 40154.

4. Irizarry, R.A., et al., Exploration, normalization, and summaries of high density oligonucleotide array probe level data. Biostatistics, 2003. 4(2): p. 249-264.

5. Clough, E. and T. Barrett, The Gene Expression Omnibus Database. Methods Mol Biol, 2016. 1418: p. 93-110.

6. Smyth, G.K., Limma: linear models for microarray data, in Bioinformatics and computational biology solutions using R and Bioconductor. 2005, Springer. p. 397-420.

7. Berger, J.A., et al., Optimized LOWESS normalization parameter selection for DNA microarray data. BMC bioinformatics, 2004. 5(1): p. 194.

8. Langfelder, P. and S. Horvath, WGCNA: an R package for weighted correlation network analysis. BMC bioinformatics, 2008. 9(1): p. 559.

9. Kanehisa, M. and S. Goto, KEGG: kyoto encyclopedia of genes and genomes. Nucleic Acids Res, 2000. 28(1): p. 27-30.

10. Liberzon, A., et al., The Molecular Signatures Database (MSigDB) hallmark gene set collection. Cell Syst, 2015. 1(6): p. 417-425.

11. Parikshak, N.N., et al., Integrative functional genomic analyses implicate specific molecular pathways and circuits in autism. Cell, 2013. 155(5): p. 1008-1021.

12. Gandal, M.J., et al., Shared molecular neuropathology across major psychiatric disorders parallels polygenic overlap. Science, 2018. 359(6376): p. 693-697.

13. Langfelder, P., B. Zhang, and S. Horvath, Defining clusters from a hierarchical cluster tree: the Dynamic Tree Cut package for R. Bioinformatics, 2007. 24(5): p. 719-720.

Supplementary Figure S1. Soft Threshold Power (Hyper-parameter) of Co-Expression Network (rWGCNA). rWGCNA, robust version of Weighted Gene Co-Expression Network Analysis

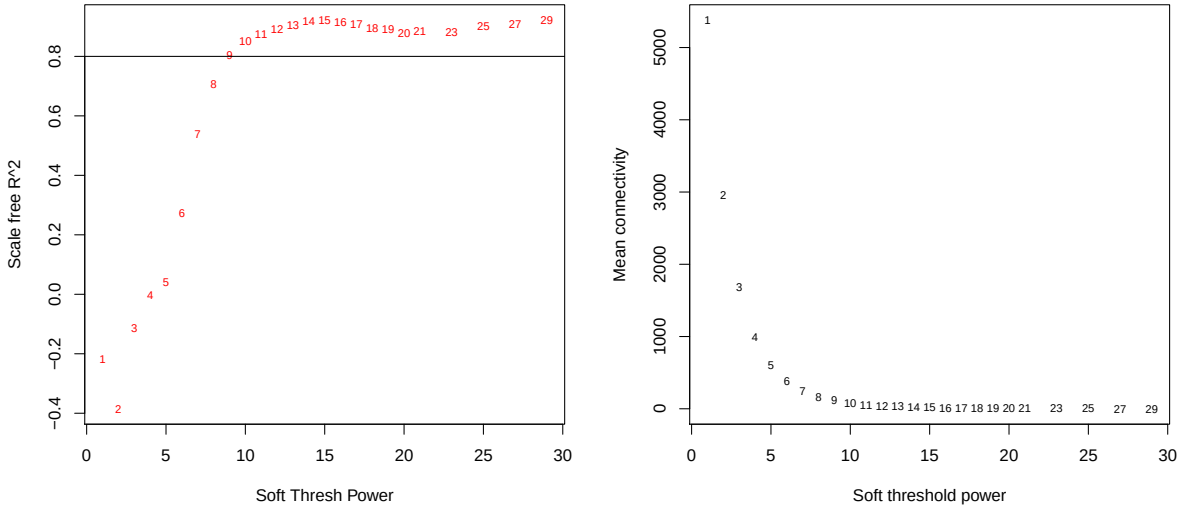

Supplementary Figure S2. DS, MMS, DCOR, PAM (Hyper-parameters) of Co-Expression Network (rWGCNA). DS, deepsplit; MMS, minimum module size; DCOR, consensus quantile threshold, PAM, pamStage; rWGCNA, robust version of Weighted Gene Co-Expression Network Analysis

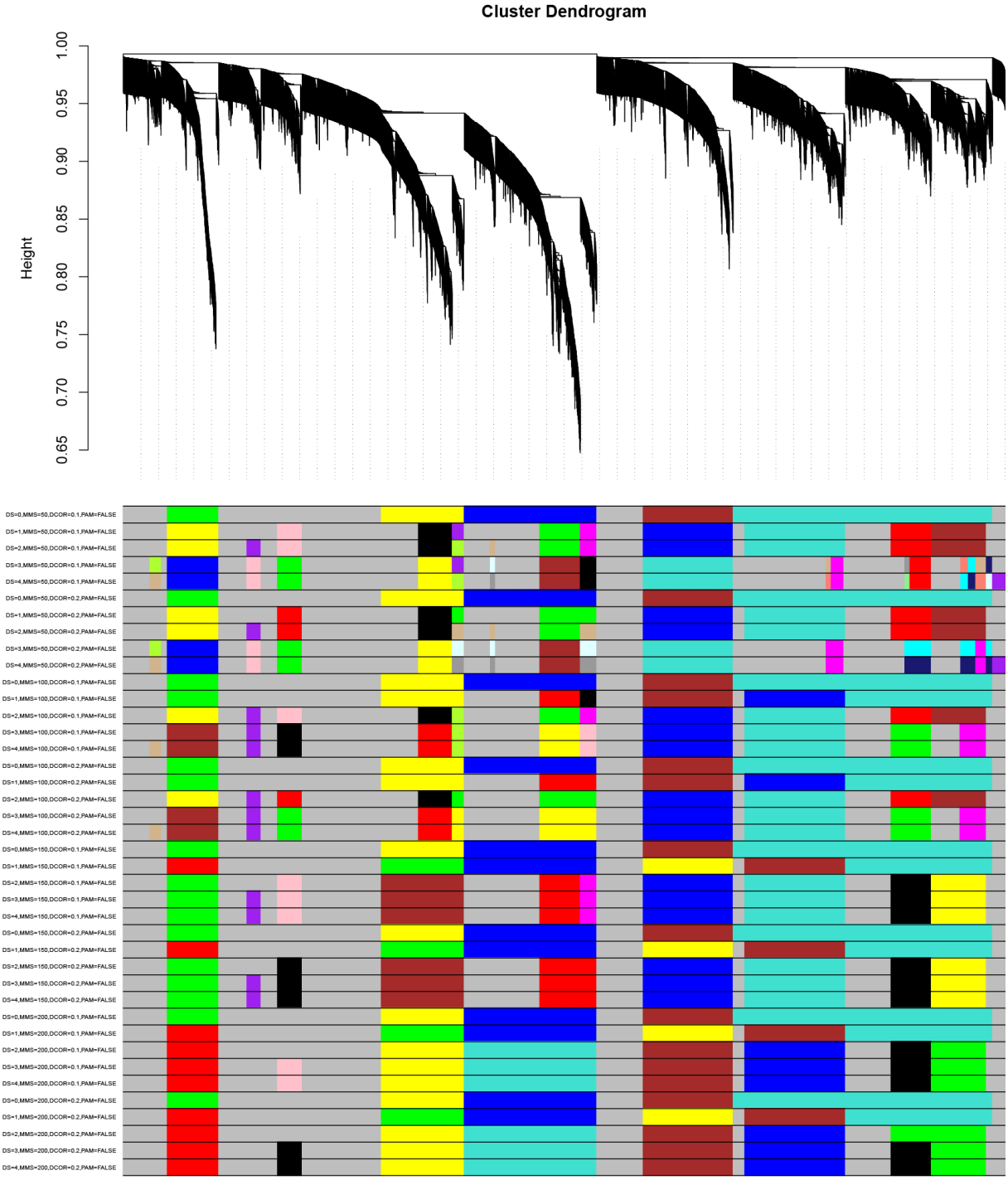

Supplementary Figure S3. Correlation matrices from Spearman correlation for all pairwise compar-isons among blood datasets in each disease. AD, Alzheimer's Disease; DM, diabetes mellitus

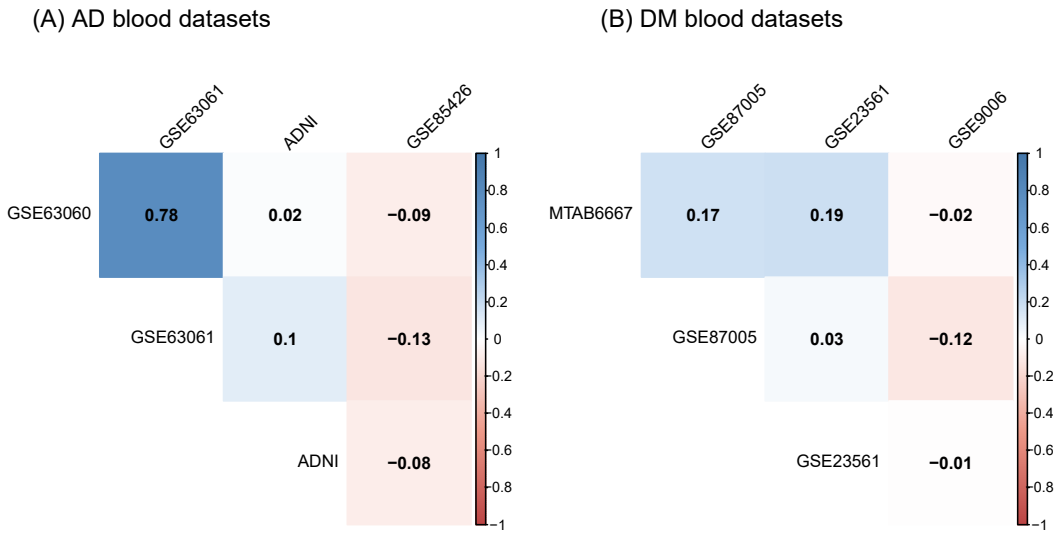

Supplementary Figure S4. Comparison of gene expressions between integrated AD blood and inte-grated DM blood datasets.

We integrated ADNI, GSE63060, GSE63061, and GSE85426 into one large AD dataset, and E-MTABL-6667, GSE87005, and GSE23561 into one large DM dataset. The number of genes that is commonly present in the seven gene expression datasets were 1,116.

AD, Alzheimer's Disease; DM, diabetes mellitus; SCC, Spearman's correlation coefficient, FC, fold change

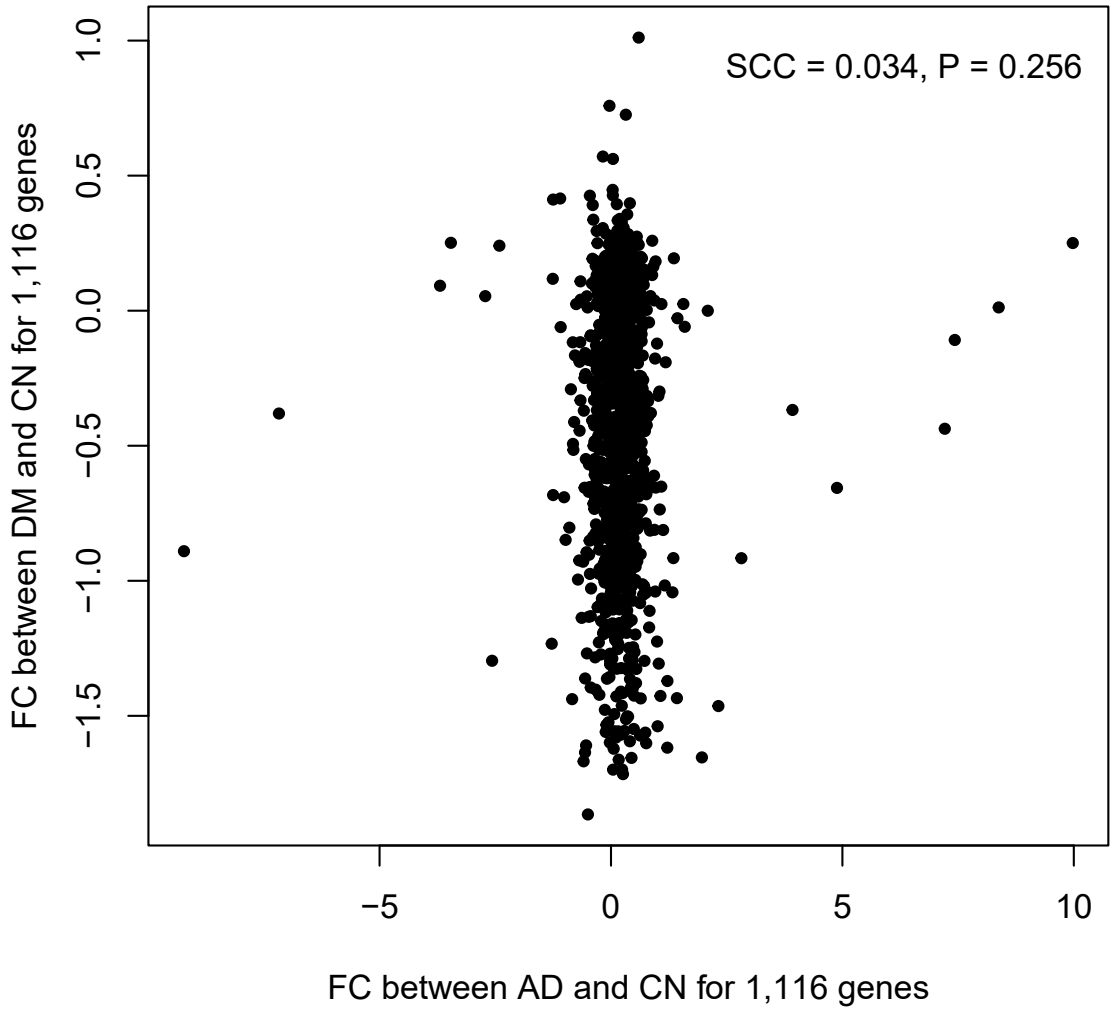

Supplementary Table S1. All analyzed datasets (AD and DM)

AD datasets				
	# of controls	# of patients	Platform	Tissue type
GSE63060	104	145	Illumina HumanHT-12 V3.0 expression beadchip (GPL6947)	blood
GSE63061	134	139	Illumina HumanHT-12 V4.0 expression beadchip (GPL10558)	blood
GSE85426	90	90	Agilent-028004 SurePrint G3 Human GE 8x60K Microarray (GPL14550)	blood
ADNI	136	63	Affymetrix Human Genome U219 Array	blood
GSE5281	74	87	Affymetrix Human Genome U133 Plus 2.0 Array (GPL570)	brain
DM datasets				
	# of control	# of patients	Platform	Tissue type
E-MTAB-6667	40	19	Illumina HumanHT-12 v4.0 (A-MEXP-2072)	blood (used), colon (not-used)
GSE87005	20	20	Agilent-014850 Whole Human Genome Microarray 4x44K G4112F (GPL6480)	blood
GSE23561	9	8	Human 50K Exonic Evidence-Based Oligonucleotide array (GPL10775)	blood
GSE9006	24	12	Affymetrix Human Genome U133B Array (GPL97)	blood
GSE81608	6 (651 cells)	12 (919 cells)	Illumina HiSeq 2500 (Homo sapiens)	pancreas (single-cell)
GSE20966	10	10	Affymetrix Human X3P Array	pancreas

AD, Alzheimer's disease; DM, diabetes mellitus

Words in brackets (Platform column) indicate datasets consisting of probes or probe-sets ID and Entrez ID.

Supplementary Table S2. Enriched pathways of genes in green module

GOID	Term	Count	FDR
GO:0006412	translation	74	<0.001
GO:0043043	peptide biosynthetic process	74	<0.001
GO:0022613	ribonucleoprotein complex biogenesis	62	<0.001
GO:0006614	SRP-dependent cotranslational protein targeting to membrane	32	<0.001
GO:0043604	amide biosynthetic process	74	<0.001
GO:0006613	cotranslational protein targeting to membrane	32	<0.001
GO:0042254	ribosome biogenesis	51	<0.001
GO:0045047	protein targeting to ER	32	<0.001
GO:0072599	establishment of protein localization to endoplasmic reticulum	32	<0.001
GO:0006518	peptide metabolic process	76	<0.001
GO:0000184	nuclear-transcribed mRNA catabolic process, nonsense-mediated decay	33	<0.001
GO:0016071	mRNA metabolic process	68	<0.001
GO:0006413	translational initiation	38	<0.001
GO:0043603	cellular amide metabolic process	82	<0.001
GO:0006396	RNA processing	78	<0.001
GO:0070972	protein localization to endoplasmic reticulum	32	<0.001
GO:0034641	cellular nitrogen compound metabolic process	248	<0.001
GO:0000956	nuclear-transcribed mRNA catabolic process	38	<0.001
GO:0016072	rRNA metabolic process	43	<0.001
GO:0006364	rRNA processing	42	<0.001
GO:0006402	mRNA catabolic process	38	<0.001
GO:1901564	organonitrogen compound metabolic process	124	<0.001
GO:0006807	nitrogen compound metabolic process	254	<0.001
GO:0006401	RNA catabolic process	39	<0.001
GO:1901566	organonitrogen compound biosynthetic process	92	<0.001
GO:0006612	protein targeting to membrane	34	<0.001
GO:0019080	viral gene expression	34	<0.001
GO:0019083	viral transcription	33	<0.001
GO:0044033	multi-organism metabolic process	34	<0.001
GO:0010467	gene expression	205	<0.001
GO:1902582	single-organism intracellular transport	59	<0.001
GO:0034470	ncRNA processing	45	<0.001
GO:0034660	ncRNA metabolic process	53	<0.001
GO:0072594	establishment of protein localization to organelle	57	<0.001
GO:0034655	nucleobase-containing compound catabolic process	42	<0.001
GO:0070125	mitochondrial translational elongation	22	<0.001
GO:0006415	translational termination	23	<0.001
GO:0070126	mitochondrial translational termination	22	<0.001
GO:0019439	aromatic compound catabolic process	44	<0.001
GO:0046700	heterocycle catabolic process	43	<0.001
GO:0006414	translational elongation	26	<0.001
GO:0044265	cellular macromolecule catabolic process	68	<0.001
GO:0033365	protein localization to organelle	65	<0.001
GO:0044270	cellular nitrogen compound catabolic process	43	<0.001
GO:0044237	cellular metabolic process	311	<0.001
GO:0006605	protein targeting	55	<0.001
GO:0046907	intracellular transport	89	<0.001
GO:1901361	organic cyclic compound catabolic process	43	<0.001
GO:0032543	mitochondrial translation	23	<0.001
GO:0090150	establishment of protein localization to membrane	38	<0.001
GO:0046483	heterocycle metabolic process	210	<0.001
GO:0006139	nucleobase-containing compound metabolic process	206	<0.001
GO:0006725	cellular aromatic compound metabolic process	210	<0.001
GO:0006886	intracellular protein transport	65	<0.001
GO:1901360	organic cyclic compound metabolic process	214	<0.001
GO:0019058	viral life cycle	40	<0.001
GO:0008152	metabolic process	321	<0.001
GO:0009057	macromolecule catabolic process	68	<0.001
GO:0007005	mitochondrion organization	47	<0.001
GO:0043624	cellular protein complex disassembly	25	<0.001
GO:0016032	viral process	59	<0.001
GO:0044260	cellular macromolecule metabolic process	261	<0.001
GO:0044764	multi-organism cellular process	59	<0.001
GO:0044267	cellular protein metabolic process	176	<0.001
GO:0044238	primary metabolic process	301	<0.001

Supplementary Table S2. Enriched pathways of genes in green module, continued

GOID	Term	Count	FDR
GO:0051649	establishment of localization in cell	93	<0.001
GO:0034613	cellular protein localization	80	<0.001
GO:0044419	interspecies interaction between organisms	59	<0.001
GO:0044403	symbiosis, encompassing mutualism through parasitism	59	<0.001
GO:0044085	cellular component biogenesis	120	<0.001
GO:0070727	cellular macromolecule localization	80	<0.001
GO:0044248	cellular catabolic process	80	<0.001
GO:0044271	cellular nitrogen compound biosynthetic process	175	<0.001
GO:0043933	macromolecular complex subunit organization	106	<0.001
GO:0072657	protein localization to membrane	38	<0.001
GO:0071704	organic substance metabolic process	308	<0.001
GO:0022904	respiratory electron transport chain	18	<0.001
GO:0000375	RNA splicing, via transesterification reactions	29	<0.001
GO:0051641	cellular localization	107	<0.001
GO:1902580	single-organism cellular localization	61	<0.001
GO:0022900	electron transport chain	18	<0.001
GO:0044249	cellular biosynthetic process	202	<0.001
GO:0043241	protein complex disassembly	26	<0.001
GO:0015031	protein transport	85	<0.001
GO:0045184	establishment of protein localization	90	<0.001
GO:0032984	macromolecular complex disassembly	26	<0.001
GO:0042775	mitochondrial ATP synthesis coupled electron transport	16	<0.001
GO:0042773	ATP synthesis coupled electron transport	16	<0.001
GO:0009205	purine ribonucleoside triphosphate metabolic process	26	<0.001
GO:0042273	ribosomal large subunit biogenesis	14	<0.001
GO:0006119	oxidative phosphorylation	17	<0.001
GO:0022618	ribonucleoprotein complex assembly	23	<0.001
GO:0008380	RNA splicing	32	<0.001
GO:0009199	ribonucleoside triphosphate metabolic process	26	<0.001
GO:0009144	purine nucleoside triphosphate metabolic process	26	<0.001
GO:0009058	biosynthetic process	204	<0.001
GO:1902600	hydrogen ion transmembrane transport	17	<0.001
GO:0000398	mRNA splicing, via spliceosome	27	<0.001
GO:0000377	RNA splicing, via transesterification reactions with bulged adenosine as nucleophile	27	<0.001
GO:0071826	ribonucleoprotein complex subunit organization	23	<0.001
GO:0046034	ATP metabolic process	24	<0.001
GO:0015992	proton transport	19	<0.001
GO:0090304	nucleic acid metabolic process	173	<0.001
GO:0006818	hydrogen transport	19	<0.001
GO:0042278	purine nucleoside metabolic process	29	<0.001
GO:0034645	cellular macromolecule biosynthetic process	169	<0.001
GO:0019538	protein metabolic process	180	<0.001
GO:0009141	nucleoside triphosphate metabolic process	26	<0.001
GO:1901657	glycosyl compound metabolic process	32	<0.001
GO:0009116	nucleoside metabolic process	31	<0.001
GO:0034622	cellular macromolecular complex assembly	53	<0.001
GO:0008104	protein localization	98	<0.001
GO:0043170	macromolecule metabolic process	266	<0.001
GO:0009167	purine ribonucleoside monophosphate metabolic process	25	<0.001
GO:0009126	purine nucleoside monophosphate metabolic process	25	<0.001
GO:0016070	RNA metabolic process	158	<0.001
GO:0006397	mRNA processing	33	<0.001
GO:0051436	negative regulation of ubiquitin-protein ligase activity involved in mitotic cell cycle	13	<0.001
GO:0046128	purine ribonucleoside metabolic process	28	<0.001
GO:0009059	macromolecule biosynthetic process	171	<0.001
GO:0051439	regulation of ubiquitin-protein ligase activity involved in mitotic cell cycle	13	<0.001
GO:1904667	negative regulation of ubiquitin protein ligase activity	13	<0.001
GO:0042255	ribosome assembly	12	<0.001
GO:0045333	cellular respiration	19	<0.001
GO:0009161	ribonucleoside monophosphate metabolic process	25	<0.001
GO:0051437	positive regulation of ubiquitin-protein ligase activity involved in regulation of mitotic cell cycle transition	13	<0.001
GO:1901576	organic substance biosynthetic process	196	0.001
GO:0031145	anaphase-promoting complex-dependent catabolic process	13	0.001
GO:0071840	cellular component organization or biogenesis	196	0.001
GO:0051444	negative regulation of ubiquitin-protein transferase activity	13	0.001

Supplementary Table S2. Enriched pathways of genes in green module, continued

GOID	Term	Count	FDR
GO:0009123	nucleoside monophosphate metabolic process	25	0.001
GO:1901575	organic substance catabolic process	79	0.001
GO:0009119	ribonucleoside metabolic process	28	0.001
GO:1904668	positive regulation of ubiquitin protein ligase activity	13	0.001
GO:0015980	energy derivation by oxidation of organic compounds	23	0.001
GO:2000058	regulation of protein ubiquitination involved in ubiquitin-dependent protein catabolic process	14	0.002
GO:0061024	membrane organization	51	0.002
GO:1904666	regulation of ubiquitin protein ligase activity	13	0.002
GO:0051443	positive regulation of ubiquitin-protein transferase activity	14	0.002
GO:0022411	cellular component disassembly	32	0.002
GO:0006091	generation of precursor metabolites and energy	27	0.003
GO:0044802	single-organism membrane organization	45	0.003
GO:0009056	catabolic process	81	0.003
GO:2000060	positive regulation of protein ubiquitination involved in ubiquitin-dependent protein catabolic process	13	0.003
GO:0009987	cellular process	386	0.005
GO:0033036	macromolecule localization	103	0.005
GO:0006120	mitochondrial electron transport, NADH to ubiquinone	10	0.008
GO:0071822	protein complex subunit organization	69	0.01
GO:0051438	regulation of ubiquitin-protein transferase activity	14	0.01
GO:0042776	mitochondrial ATP synthesis coupled proton transport	7	0.015
GO:0016043	cellular component organization	186	0.016
GO:0031397	negative regulation of protein ubiquitination	14	0.024
GO:0007346	regulation of mitotic cell cycle	29	0.032
GO:0032981	mitochondrial respiratory chain complex I assembly	10	0.033
GO:0010257	NADH dehydrogenase complex assembly	10	0.033
GO:0097031	mitochondrial respiratory chain complex I biogenesis	10	0.033
GO:1901990	regulation of mitotic cell cycle phase transition	22	0.033
GO:0071702	organic substance transport	95	0.035
GO:0065003	macromolecular complex assembly	68	0.036
GO:1903322	positive regulation of protein modification by small protein conjugation or removal	17	0.038
GO:0006996	organelle organization	124	0.045
GO:0030529	intracellular ribonucleoprotein complex	102	<0.001
GO:1990904	ribonucleoprotein complex	102	<0.001
GO:0044391	ribosomal subunit	55	<0.001
GO:0005840	ribosome	59	<0.001
GO:0032991	macromolecular complex	234	<0.001
GO:0044446	intracellular organelle part	309	<0.001
GO:0044422	organelle part	310	<0.001
GO:0015934	large ribosomal subunit	37	<0.001
GO:0022626	cytosolic ribosome	36	<0.001
GO:0043229	intracellular organelle	373	<0.001
GO:0043227	membrane-bounded organelle	374	<0.001
GO:0043231	intracellular membrane-bounded organelle	353	<0.001
GO:0070013	intracellular organelle lumen	196	<0.001
GO:0044424	intracellular part	397	<0.001
GO:0031974	membrane-enclosed lumen	198	<0.001
GO:0043233	organelle lumen	196	<0.001
GO:0005622	intracellular	400	<0.001
GO:0005740	mitochondrial envelope	69	<0.001
GO:0031966	mitochondrial membrane	67	<0.001
GO:0005743	mitochondrial inner membrane	57	<0.001
GO:0043226	organelle	384	<0.001
GO:0019866	organelle inner membrane	59	<0.001
GO:0044445	cytosolic part	40	<0.001
GO:0044444	cytoplasmic part	282	<0.001
GO:0005739	mitochondrion	105	<0.001
GO:0044429	mitochondrial part	77	<0.001
GO:0022625	cytosolic large ribosomal subunit	23	<0.001
GO:0031981	nuclear lumen	161	<0.001
GO:0044428	nuclear part	169	<0.001
GO:0005737	cytoplasm	330	<0.001
GO:0031967	organelle envelope	77	<0.001
GO:0031975	envelope	77	<0.001
GO:0005829	cytosol	148	<0.001
GO:0000313	organellar ribosome	21	<0.001

Supplementary Table S2. Enriched pathways of genes in green module, continued

GOID	Term	Count	FDR
GO:0005761	mitochondrial ribosome	21	<0.001
GO:0005634	nucleus	240	<0.001
GO:0043228	non-membrane-bounded organelle	162	<0.001
GO:0043232	intracellular non-membrane-bounded organelle	162	<0.001
GO:0044455	mitochondrial membrane part	29	<0.001
GO:0015935	small ribosomal subunit	19	<0.001
GO:0098800	inner mitochondrial membrane protein complex	24	<0.001
GO:0098798	mitochondrial protein complex	26	<0.001
GO:0005654	nucleoplasm	126	<0.001
GO:0005762	mitochondrial large ribosomal subunit	14	<0.001
GO:0000315	organellar large ribosomal subunit	14	<0.001
GO:0005730	nucleolus	55	<0.001
GO:0005759	mitochondrial matrix	36	<0.001
GO:0043234	protein complex	153	<0.001
GO:0070469	respiratory chain	17	<0.001
GO:0022627	cytosolic small ribosomal subunit	13	<0.001
GO:0016469	proton-transporting two-sector ATPase complex	13	<0.001
GO:0005746	mitochondrial respiratory chain	16	<0.001
GO:0071013	catalytic step 2 spliceosome	16	<0.001
GO:0098803	respiratory chain complex	15	<0.001
GO:0031090	organelle membrane	106	<0.001
GO:0070062	extracellular exosome	109	<0.001
GO:1903561	extracellular vesicle	109	<0.001
GO:0043230	extracellular organelle	109	<0.001
GO:0005753	mitochondrial proton-transporting ATP synthase complex	9	<0.001
GO:0045259	proton-transporting ATP synthase complex	9	<0.001
GO:0005681	spliceosomal complex	19	<0.001
GO:1902494	catalytic complex	54	<0.001
GO:0044464	cell part	405	0.001
GO:0030532	small nuclear ribonucleoprotein complex	11	0.001
GO:0005623	cell	405	0.001
GO:0097525	spliceosomal snRNP complex	10	0.004
GO:0005747	mitochondrial respiratory chain complex I	9	0.011
GO:0045271	respiratory chain complex I	9	0.011
GO:0030964	NADH dehydrogenase complex	9	0.011
GO:0005763	mitochondrial small ribosomal subunit	7	0.013
GO:0000314	organellar small ribosomal subunit	7	0.013
GO:0000502	proteasome complex	10	0.014
GO:1990234	transferase complex	37	0.014
GO:1990204	oxidoreductase complex	12	0.027
GO:0031988	membrane-bounded vesicle	117	0.037
GO:0003735	structural constituent of ribosome	50	<0.001
GO:0003723	RNA binding	122	<0.001
GO:0044822	poly(A) RNA binding	99	<0.001
GO:0005198	structural molecule activity	55	<0.001
GO:0003676	nucleic acid binding	146	0.001
GO:0015078	hydrogen ion transmembrane transporter activity	16	0.001
GO:0050136	NADH dehydrogenase (quinone) activity	10	0.014
GO:0003954	NADH dehydrogenase activity	10	0.014
GO:0008137	NADH dehydrogenase (ubiquinone) activity	10	0.014
GO:0016655	oxidoreductase activity, acting on NAD(P)H, quinone or similar compound as acceptor	11	0.014
hsa03010	Ribosome	43	<0.001
hsa00190	Oxidative phosphorylation	28	<0.001
hsa05010	Alzheimer's disease	22	<0.001
hsa05012	Parkinson's disease	20	<0.001
hsa05016	Huntington's disease	21	0.003
hsa03040	Spliceosome	17	0.004
TF	RPS27A, MTERF3, RPL7, SSB, RIOK2, PHF5A, GTF2F2, CEBPG, ZMAT2, PUM3, LARP7, ZNF17, POLE4, ZNF613, ZNF26, CGGBP1, ZNF22, ZNF302, PSMD10, BCLAF1, ZNF277, S100A8, THAP12, GPBP1, PAX7, CEBPZ, ZNF816, COPS4, GTF2B, GTF2E2, COMMD6, SUB1, PSMA6, TCEAL8, ZBED5, MYNN, SLC30A9, TAX1BP1, CNBP, ZC3H15, BOLA2	NA	